

Supplemental information for:  
Experimental investigation of photo-  
thermal catalytic reactor for the reverse  
water gas shift reaction under  
concentrated irradiation

David Brust<sup>a</sup>, Michael Wullenkord<sup>a</sup>, Hermenegildo García Gómez<sup>b</sup>,  
Josep Albero<sup>b</sup>, Christian Sattler<sup>a</sup>

<sup>a</sup>German Aerospace Center (DLR) - Institute of Future Fuels, Linder Höhe, 51147 Köln, Germany

<sup>b</sup>Instituto Universitario de Tecnología Química (CSIC-UPV), Universitat Politècnica de València,  
Avda. De los Naranjos, Valencia 46022, Spain

## 1. Catalyst deposition on porous frit

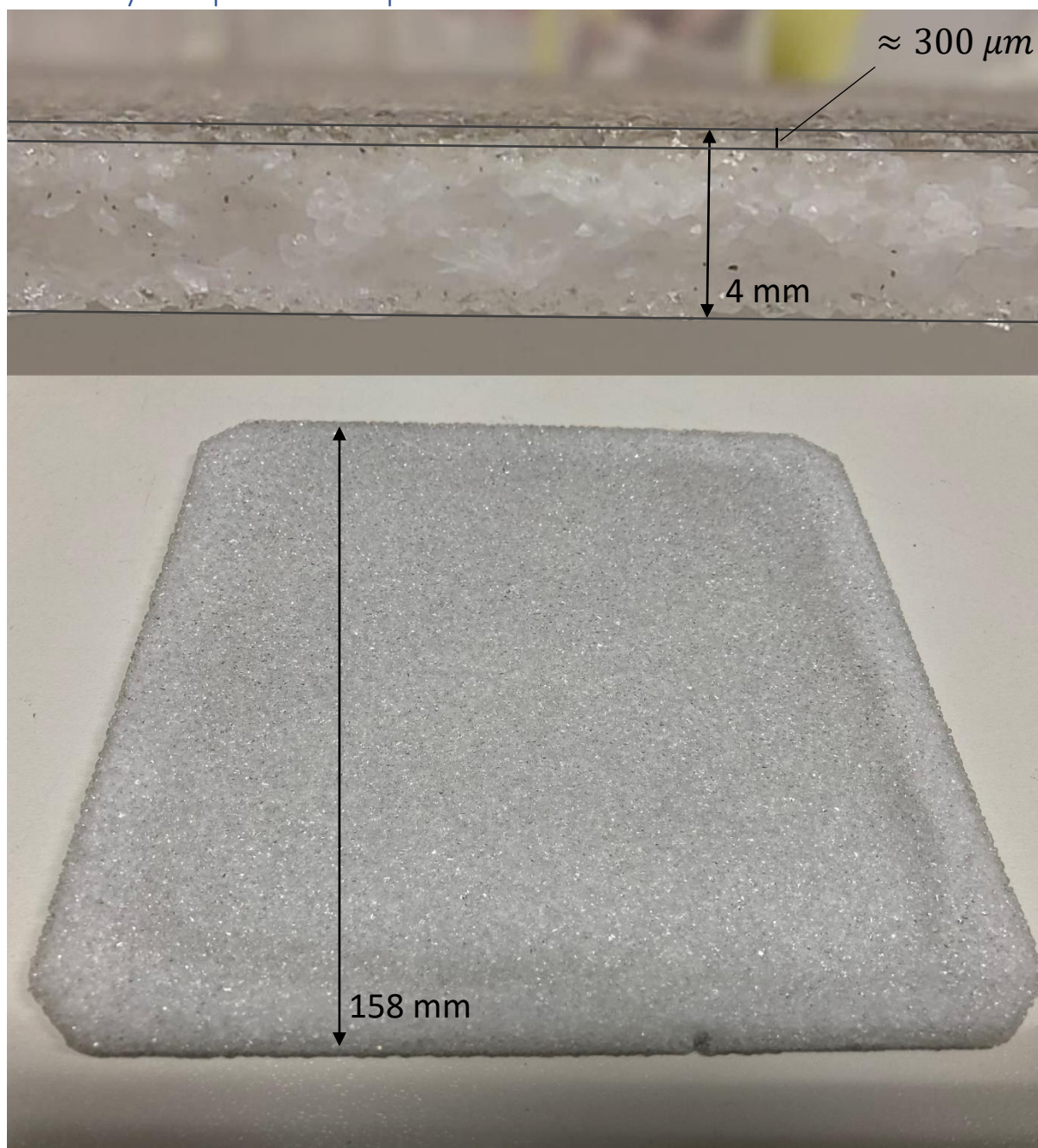


Figure S 1: Images of both the cross-section (upper image) and the surface (bottom picture) of the porous quartz supporting the catalyst

## 2. Mounting and assembly of the reactor

The reactor was mounted vertically (Figure S 2 a) directly behind the flux guide (not shown in Figure S 2). Two methods of catalyst deposition were realised: deposition on glass-fibre membrane sheets (Figure S 2 b) and directly on the porous frit made of sintered glass (Figure S 2 c).

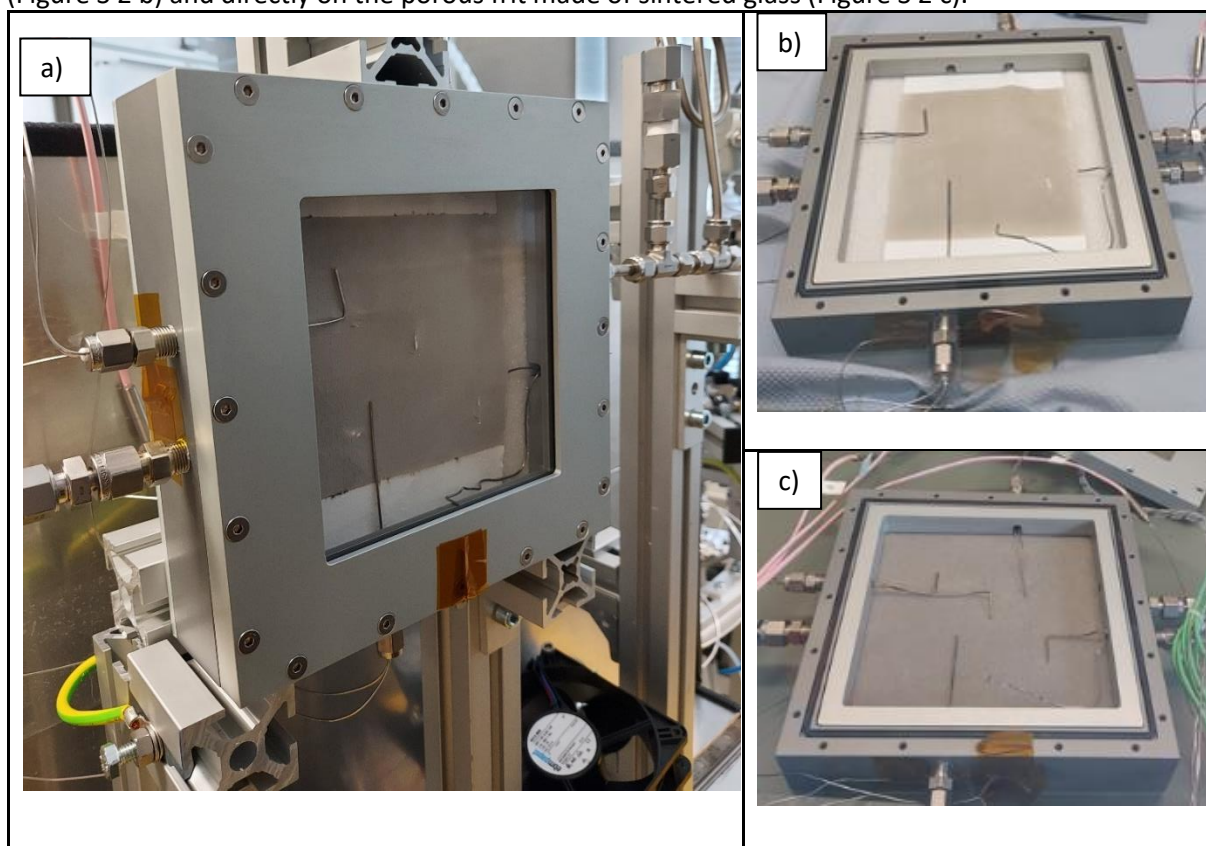


Figure S 2: Photo-thermal catalytic reactor – a) Assembled and mounted reactor including gas connections and thermocouples; disassembled reactor with catalyst on b) glass fibre sheet and c) porous glass frit

### 3. Reflectance spectra at different temperatures

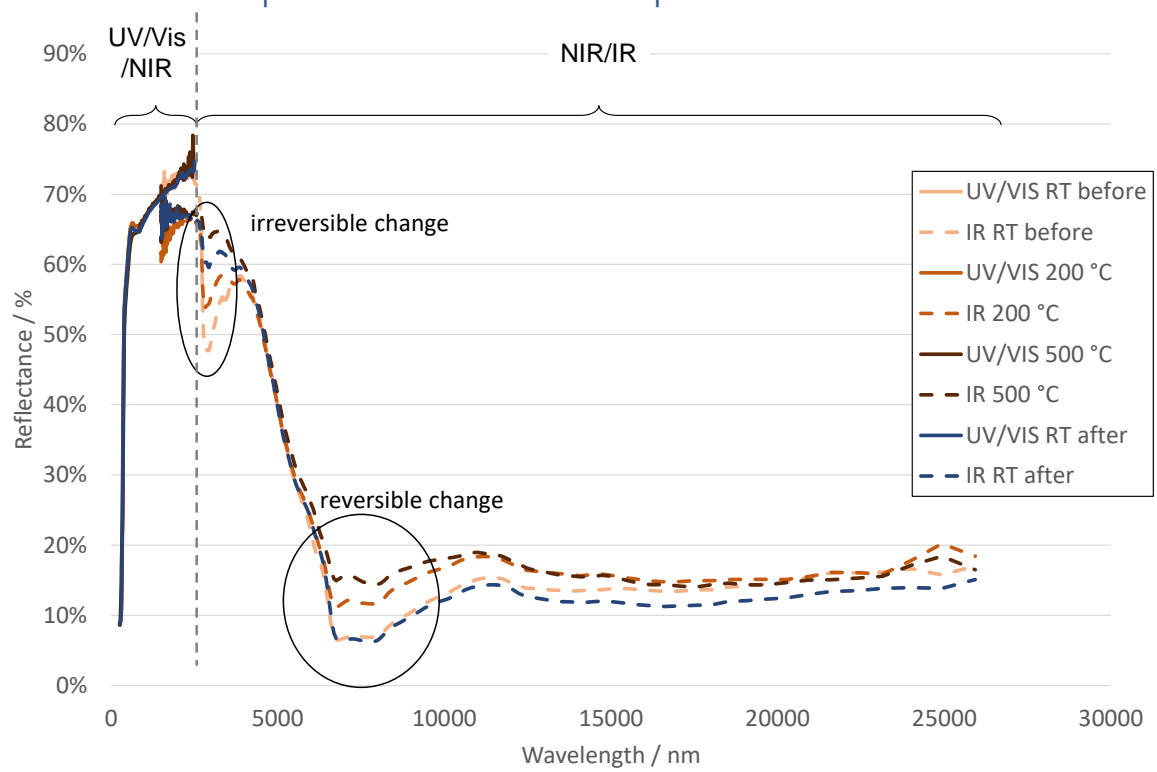


Figure S 3: Reflectance spectra of the RuO<sub>2</sub>-SrTiO<sub>3</sub> catalyst deposited on glass fibre sheets with a mass loading of 10 mg/cm<sup>2</sup> in the spectral range from 250 nm to 25000 nm at room temperature, 200 °C and 500 °C respectively, contrasting spectra before and after the heating process that was part of measurement.

### 4. Piping and instrumentation diagram

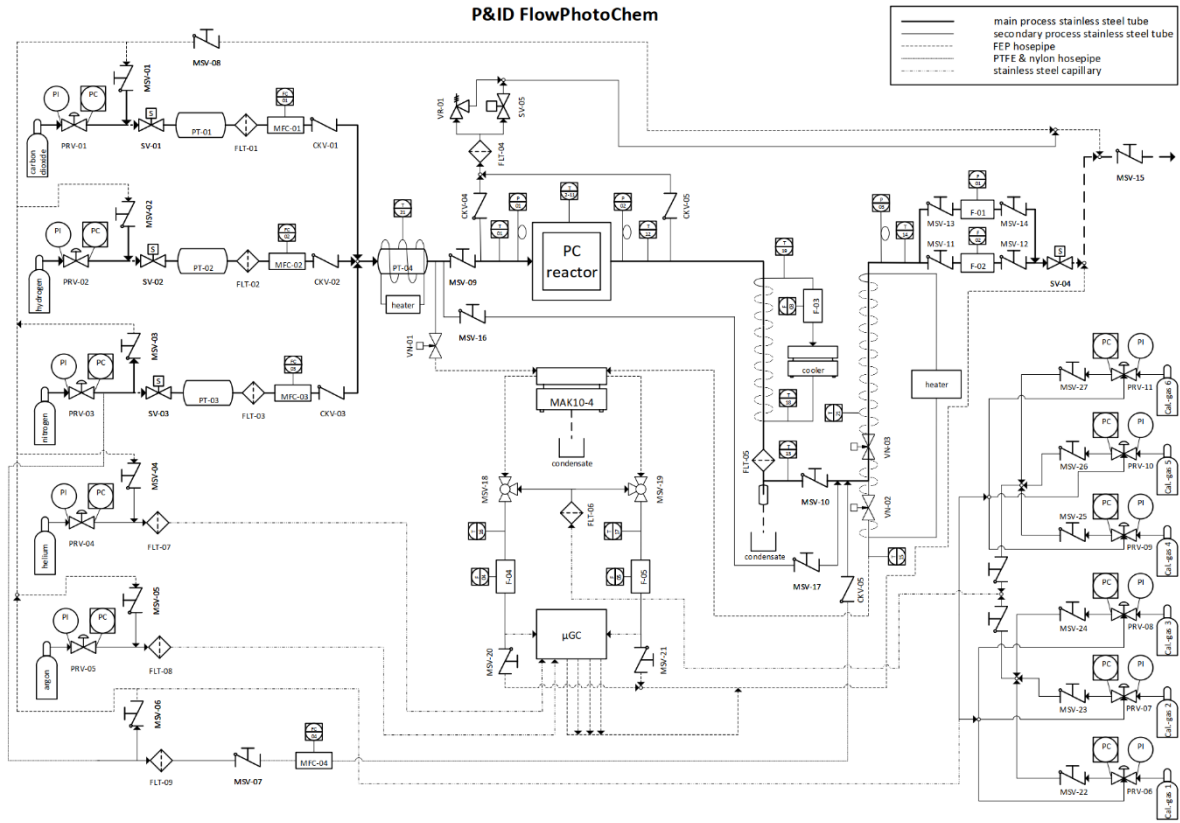


Figure S 4: Complete P&ID of the test setup with the reactor in the centre. The P&ID also features the gas feed, exhaust, gas analysis and preconditioning as well as implements for calibration.

## 5. Measurement positions for temperature

Temperature measurements were performed inside and outside the photo-thermal catalytic reactor. In the upper reactor chamber, where the irradiated catalyst layer resides, there are 9 thermocouples. The lower chamber is equipped with 4 thermocouples, combined with 4 additional thermocouples at various positions outside the reactor this leads to 17 measurement positions for temperature in total at the reactor.

The placement can be seen according to the schematic in Figure S 5 in the upper chamber and in Figure S 6 the lower chamber.

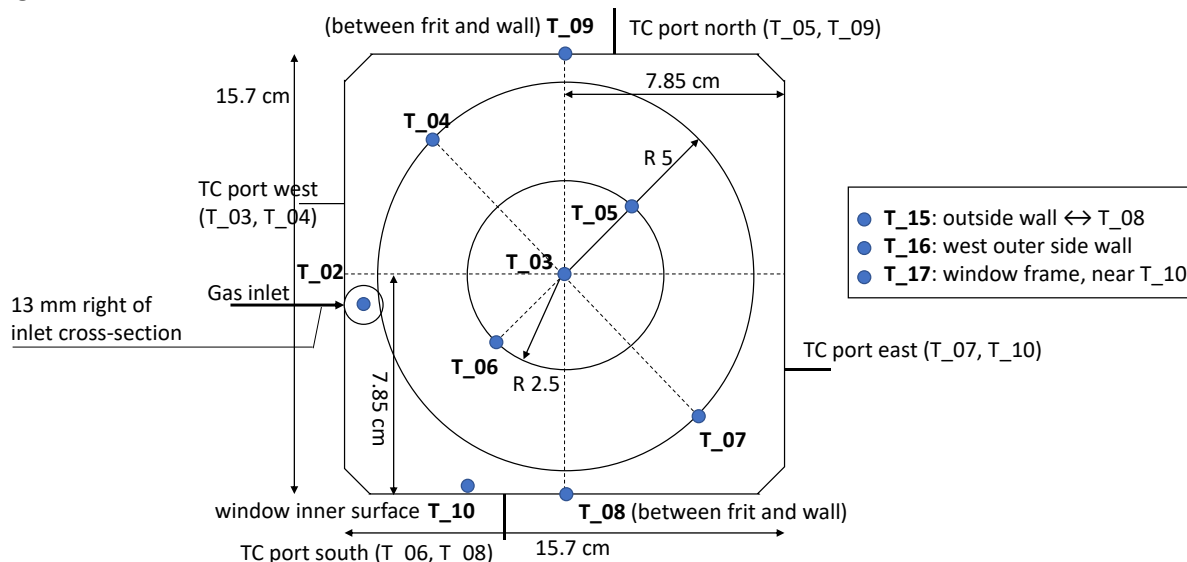


Figure S 5: Schematic sketch of upper chamber of the photo-thermal catalytic reactor showing the placement and naming convention of thermocouples close to the front surface of the frit.

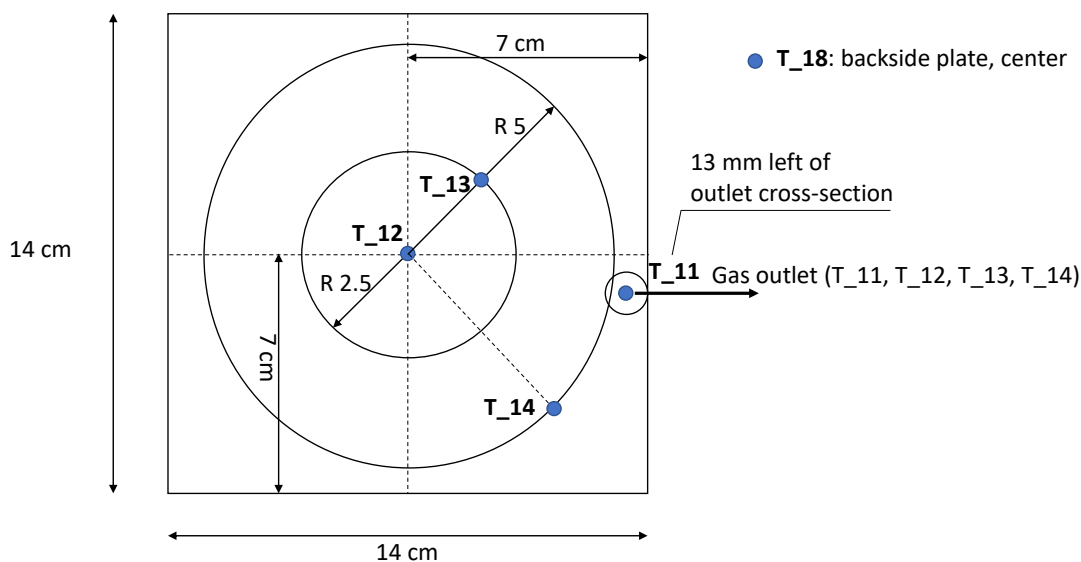


Figure S 6: Schematic sketch of lower chamber of the photo-thermal catalytic reactor showing the placement and naming convention of thermocouples close to the back surface of the frit.

## 7. Additional Flux Profiles

The solar simulator was qualified for the nominal fluxes on the catalyst core area of the central 10 cm x 10 cm with 40, 60, 80 and 100 kW/m<sup>2</sup>. The flux map for 40 kW/m<sup>2</sup> is shown in Figure 1 in the main text, the remaining flux maps are shown in the following.

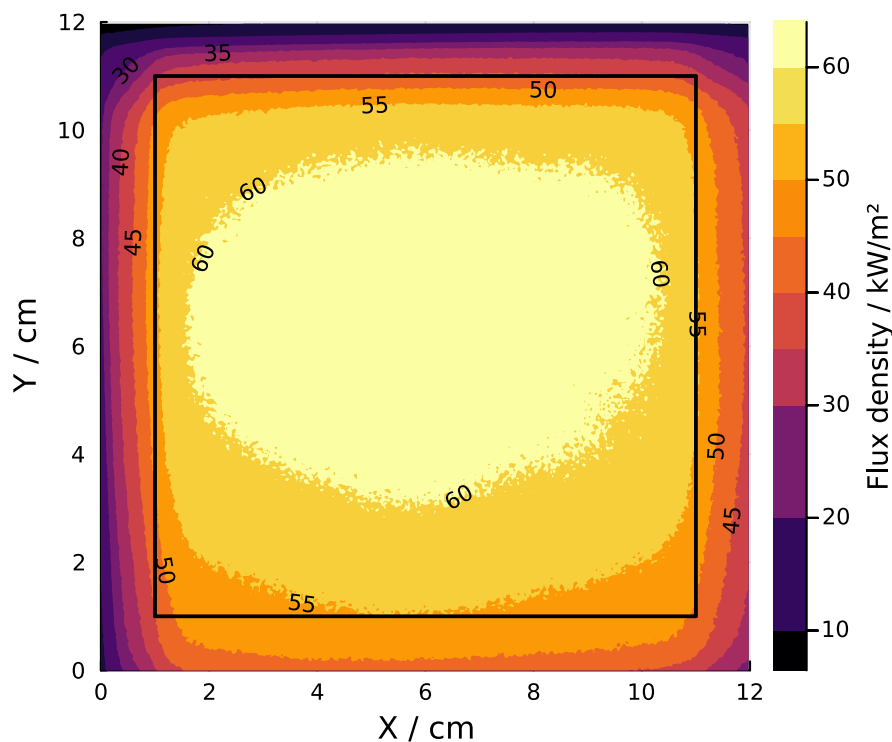


Figure S 7: Effective flux profile originally assigned to a nominal flux of 60 kW/m<sup>2</sup> on the catalyst core area corresponding to a lamp current of 124 A.

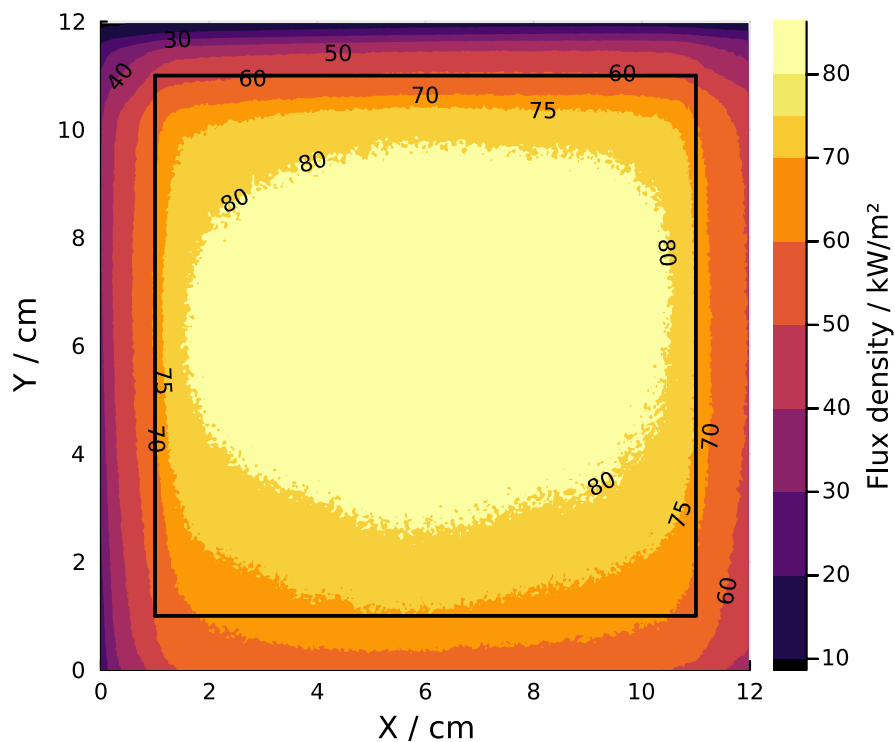


Figure S 8: Effective flux profile originally assigned to a nominal flux of 80 kW/m<sup>2</sup> on the catalyst core area corresponding to a lamp current of 147 A.





## 8. Time evolution during experiment

Exemplary results for a particular test day that considered a constant reactant flow of 3 L<sub>s</sub>/min (H<sub>2</sub>/CO<sub>2</sub> = 1/1) and a variation of the flux is shown in Figure S 10. The temperature rises with increasing flux as well as the fraction of CO in the product gas. Mean temperatures recorded by the directly irradiated thermocouples on the catalyst surface of 472-675°C were determined. The data shown in Figure S 10 corresponds to the experimental data analysed in Figures 10 a) and 11 a) in the main text.

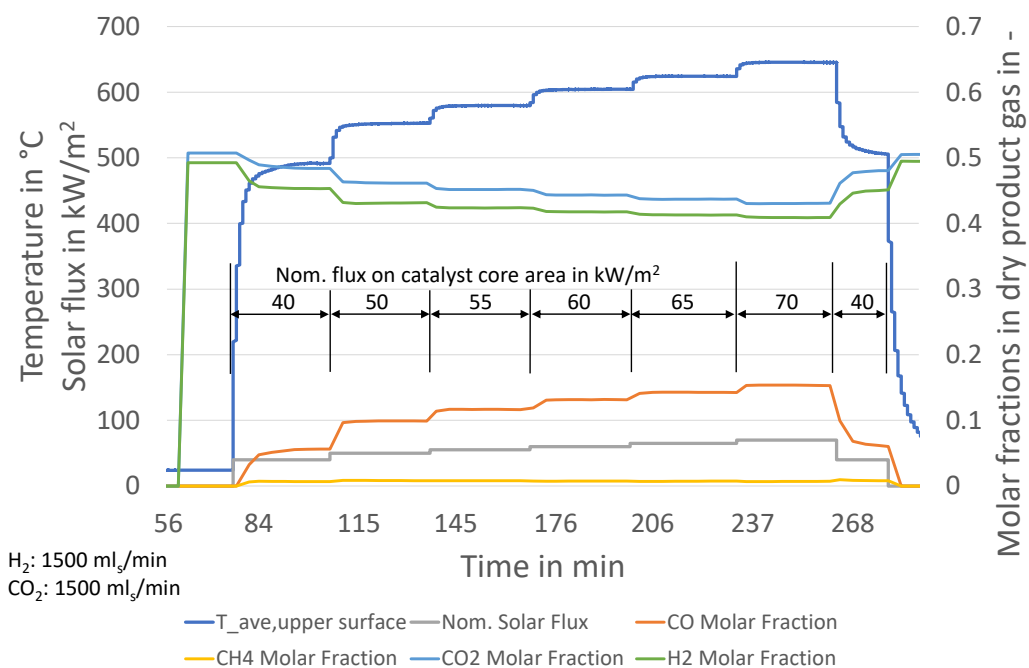


Figure S 10: Exemplary evolution of the temperature recorded by temperature sensors in contact with the upper surface of the catalyst and molar fractions in the dry product gas as a function of the irradiation conditions

## 9. Comparing temperatures from measurement and calculation

Table S 1 and Table S 2 contain the values shown in Figure 10 a) and b) in the main text, respectively.

Flux on catalyst (nominal) / kW/m <sup>2</sup>	Catalyst Temperature (calc.) / °C	Thermocouple Temperature (calc.) / °C	Thermocouple Temperature (exp.) / °C
40	463 ± 31	524 ± 27	500 ± 2.16
50	514 ± 33	583 ± 30	562 ± 2.43
55	537 ± 33	609 ± 31	590 ± 2.56
60	558 ± 32	634 ± 32	616 ± 2.66
65	576 ± 32	657 ± 32	636 ± 2.76
70	597 ± 32	682 ± 33	659 ± 2.85

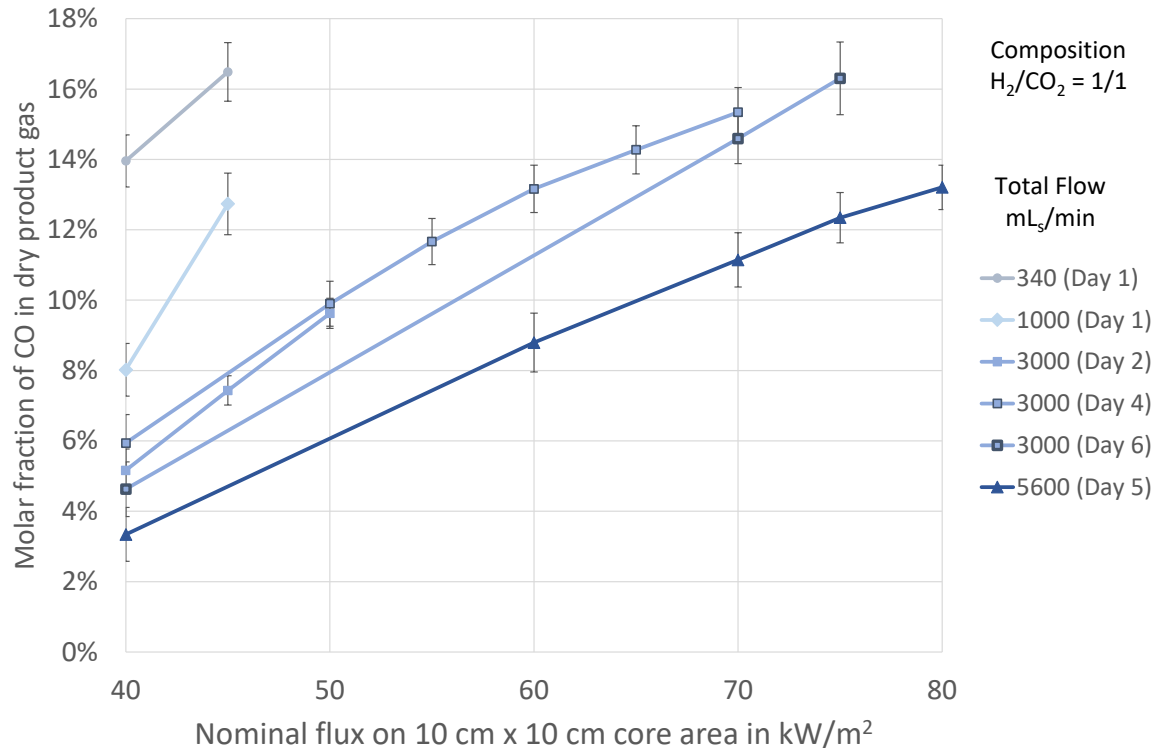
Table S 1: Calculated and experimental temperatures in the centre of the catalyst surface for constant feed flow of 3 L<sub>3</sub>/min of H<sub>2</sub>/CO<sub>2</sub> = 1/1 molar ratio at various irradiation fluxes. All reported uncertainties are standard uncertainties.

Flux on catalyst (nominal) / kW/m <sup>2</sup>	Catalyst Temperature (calc.) / °C	Thermocouple Temperature (calc.) / °C	Thermocouple Temperature (exp.) / °C
40	444 ± 29	497 ± 26	484 ± 2.10
60	539 ± 34	607 ± 31	595 ± 2.58
70	580 ± 33	656 ± 32	642 ± 2.78
75	597 ± 33	677 ± 33	668 ± 2.89
80	613 ± 33	697 ± 34	688 ± 2.98

Table S 2: Calculated and experimental temperatures in the centre of the catalyst surface for constant feed flow of 5.6 L<sub>3</sub>/min of H<sub>2</sub>/CO<sub>2</sub> = 1/1 molar ratio at various irradiation fluxes. All reported uncertainties are standard uncertainties.

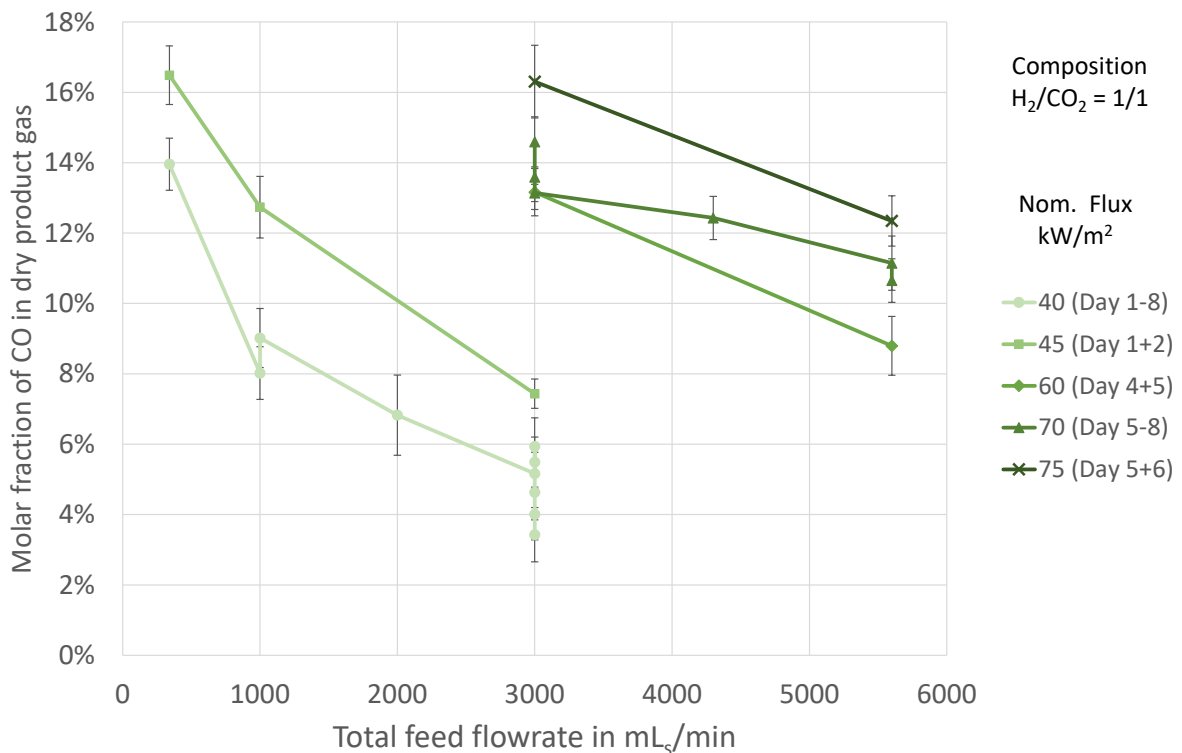
## 10. Chemical evaluation plots

Figures S 11-13 show data for molar CO fraction in the dry product gas corresponding to the data shown in Figure 12 from the main text. Therein, data recorded over the 8-day testing duration is plotted over the nominal irradiation flux density, total feed flow and feed composition (molar basis) in Figures S 11, S 12 and S 13 respectively.



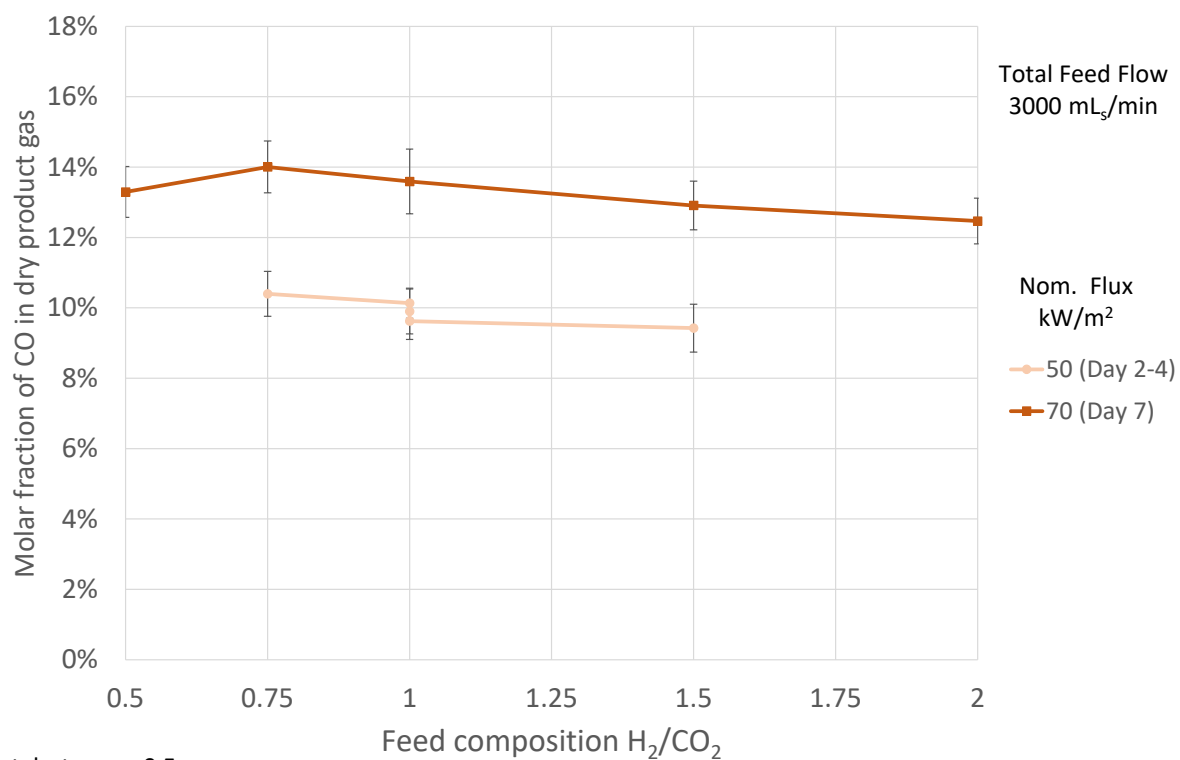
Catalyst mass: 0.5 g

Figure S 11: Molar CO fraction in dry product gas over nominal irradiation flux density for different total feed flow rates.



Catalyst mass: 0.5 g

Figure S 12: Molar CO fraction in dry product gas over total feed flowrate for different nominal irradiation flux densities.



Catalyst mass: 0.5 g

Figure S 13: Molar CO fraction in dry product gas over H<sub>2</sub>/CO<sub>2</sub> feed compositions (molar basis) for different irradiation flux densities.